JOURNAL OF MATERIALS SCIENCE 32 (1997) 1909–1914

The effects of strain annealing on grain boundaries and secure triple junctions in nickel 200

C. B. THOMSON, V. RANDLE
Department of Materials Engineering, University of Wales Swansea, Swansea SA2 8PP, UK

Changes in the microstructure of 99.5% pure nickel as a function of strain annealing have been investigated. The application of moderate amounts of compressive strain (6–7%), and subsequent thermal treatment at 750 °C under vacuum is shown to increase the density of Σ3 grain boundaries, where the coincident-site lattice rationale is adopted to characterize the boundaries. A preliminary, post-strain surface oxidation treatment to 500 °C is shown to drastically increase the proportion of twin boundaries, a majority of which are identified as being coherent in nature. In addition, a high level of connectivity for these twins is observed, along with greatly increased numbers of secure triple junctions. It is postulated that the mechanism by which grain boundary energy minimization is effected involves grain rotations when treatment is conducted under vacuum, but that annealing twin formation is the predominant process when an oxygen-rich environment exists.

1. Introduction

Improving the physical and mechanical properties of materials, and thereby increasing their performance, by adapting and controlling the microstructure has been of considerable interest to materials scientists and engineers for thirty years or more. One popular method of achieving this is strain annealing. The application of moderate quantities of strain, either tensile or compressive, followed by suitable thermal treatment, has been shown [1, 2] to be effective in increasing the resistance of a material to intergranular degradation. In polycrystals, grain boundaries are regions of disorder and have an intrinsically higher associated free energy than the grains themselves, which have a more ordered structure. Hence, grain boundaries are constantly endeavouring to achieve lower energy configurations. This, however, is an activated process and so a driving force is required to overcome the barrier to energy minimization. Grain boundary geometry is governed by the atomic structures on either side of the interface, and changes in the texture, or orientation of the grains, therefore result in modifications to the grain boundary structures. Improvements in the characteristics of a material can therefore be effected by manipulating the texture. As a consequence, the grain boundary structures can, to a limited degree, be controlled, and this is of fundamental importance since most failure in service (for example, fracture [3], corrosion [4] and cavitation [5]) is associated with elements of the boundary crystallography.

Grain boundaries can be classified as low-angle boundaries (LABs), coincident-site lattice boundaries (CSLs) or random boundaries according to the misorientation of the grains, which itself is derived from the orientation of adjacent grains. The relative proportions of these boundary types contribute to the misorientation texture. The results can be interpreted with the aid of the coincident site lattice (CSL) model [6], which categorizes boundaries in terms of the maximum number of atomic positions that would be overlaid if the lattices of adjacent grains were superimposed, and labels them according to the density of these overlaid, or coincidence, sites, and the axis (*hkl*-for cubic systems) and angle (θ) of rotation required to bring the lattices into crystallographic equivalence.

A wide array of physical parameters, such as the impurity content, annealing temperature, grain size, atmosphere, and degree of pre-strain can influence the results from a strain annealing experiment, and hence a limitation on the number of experimental variables is considered judicious. In order to keep the experimental matrix as simple as possible in this work, nickel 200 (99.5% pure) was chosen as the material for study, thus avoiding any alloying effects. In addition, nickel provides a suitably low characteristic stacking fault energy, hence enabling twinning to occur readily. The presence of annealing twins has previously been shown to favourably influence the properties of materials both directly [5, 7] due to their associated low energy configuration, and indirectly [8] via their

0022–2461

TABLE 1 Details of the thermomechanical treatments applied

Sample	Strain (%)	Thermal treatment
0	None	None
1	6	None
6	6	750 °C/12 h
3	7	750 °C/24 h
2	7	750 °C/21.5 h + 750 °C/26.5 h
1A	6	500 °C/9 h + 750 °C/12 h

interaction with other boundary types to produce more low energy boundaries.

2. Experimental details

A series of thermomechanical treatments was applied to the 99.5% pure nickel specimens (Ni200). The initial microstructures were assumed to be the same, since all the samples were taken from the same sheet. Standard metallographic techniques were applied to prepare the specimens for electron backscatter diffraction (EBSD) analysis in a 6100 Jeol scanning electron microscope. Three to four hundred grains were studied for each specimen, except for the reference sample (sample 0) for which 111 grains were studied. Manipulation, via orientation matrix inversion and multiplication, allowed the boundary structures to be elucidated in terms of the CSL model.

Details of the treatments applied to each specimen are given in Table 1. Compressive strain was applied to the sample in a forge at room temperature, and set to press at a rate of 0.00833 mm per s. The initial sample dimensions were all approximately 6×4 mm, with a thickness of 2.0 mm. Rapid ramp rates were achieved by placing the samples into a pre-heated furnace, and removing immediately on completion of the required anneal. All thermal treatments were conducted under vacuum, except for sample 1A, which was treated in an air atmosphere.

Both interactive [9] and remote [10] software applications were used in the orientation/misorientation analysis. The CSL data were output as a Σ value, the proportion of the Σ-type in the grain boundary network, and the deviation from exact misorientation. In addition, grain size and microhardness measurements were made.

3. Results

The textures obtained from the EBSD grain orientation data are shown in inverse pole figure (IPF) format in Fig. 1(a–f). Compressive strain is usually associated with [110] type textures, but as can be seen from these plots there is an absence of strong [110] texture for any of the samples. This can be accounted for by noting that the applied strains are small ($\leqslant 7\%$), and that on close observation of the IPFs a weak tendency towards the [1 1 0] pole can be identified. The IPFs for samples 1 and 6 show a grouping of data points within a 5° region about the [110] pole, but this limited effect can be seen to diminish for samples 3, 2 and 1A.

There is a slight trend towards increased [100] texture with greater treatment time at 750 °C, although the texture never rises much above that for a completely random texture. A similar trend about the [111] pole can also be identified, but again this effect is weak. The IPF for sample 1A shows a far from random texture, the preferred orientation being towards the [110] pole of the standard stereographic projection.

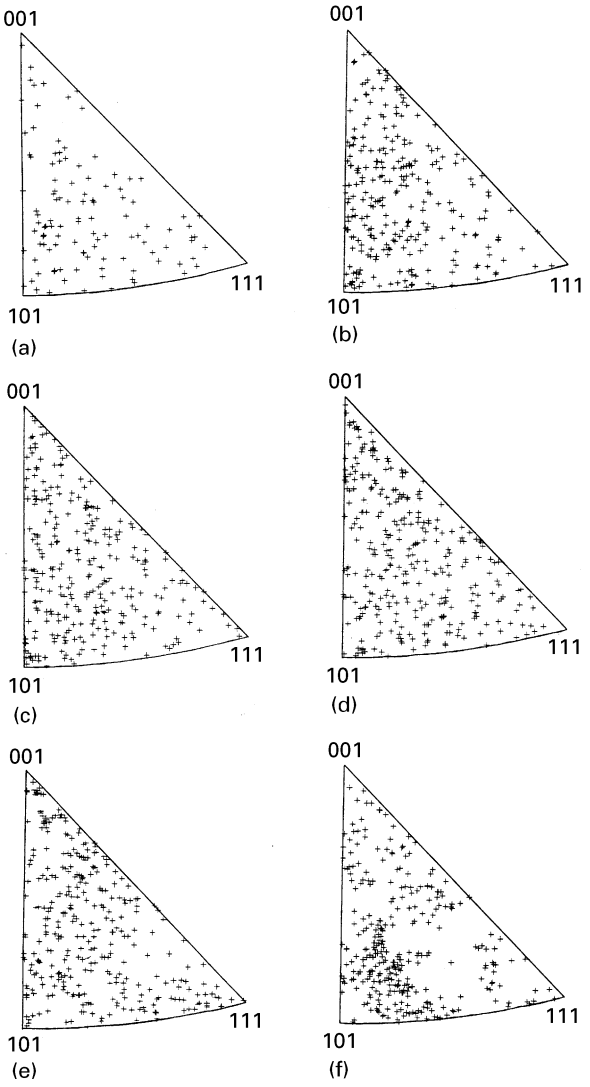

Figure 1 Inverse pole figures showing the microtextures of samples 0,1, 6, 3, 2 and 1A ((a) to (f) respectively).

The above texture changes are not accompanied by any appreciable grain growth, with the average grain sizes being 14 ± 3 μm. A consistent drop in the hardness of the samples were observed for the samples treated only at 750 °C, from 150 HV for sample 0 to 135 HV for sample 2. However, a value of 114 HV was produced for sample 1A, indicating a greater release of strain energy for this sample.

Analysis of the data output from the EBSD system allows a comparative study of the interfacial geometries to be made. Fig. 2 shows how the number densities of LAB, Σ3, Σ5, Σ7, Σ9, Σ11 and Σ13 to Σ29 CSL-types vary throughout the sample series, and compares them to values predicted for a random polycrystal [11].

Trends can be clearly seen in the LAB and Σ3 data. Increased thermal treatment has the effect of reducing

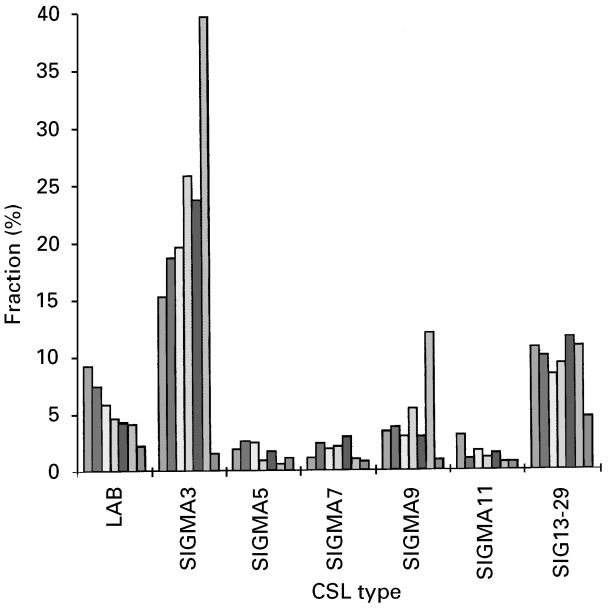

Figure 2 The fraction of selected CSL types in each sample, compared to the fraction in a random polycrystal for (■) Sample ○, (■) Sample 1, (□) Sample 6, (□) Sample 3, (■) Sample 2, (□) Sample 1A and (■) random.

the numbers of LABs, although the random distribution level is never quite reached. The numbers of Σ3 boundaries increase steadily with increased treatment time at 750 °C, up to a maximum at 24 h, from an initial value well above the random prediction. Further treatment at this temperature does not serve to increase the proportion of these boundary types, and it can therefore be assumed that the driving force provided to the system by the compressive strain has been expended. A dramatic increase in the Σ3 density can be observed for sample 1A, about 40% of the total number of boundaries sampled being of this type. It is clear that a thermal treatment for 9 h at 500 °C followed by 12 h at 750 °C brings about a stronger misorientation texture than treatment solely at 750 °C. There are no strong trends in the data for the other CSL-types, but the number of Σ9s (crystallographically related to Σ3 [12]) for sample 3 and 1A are greater than for the rest of the sample series.

4. Discussion

For a grain boundary to provide an obstacle to, for example, the propagation of a crack through a material, it must have special properties. A majority of the boundaries in a randomly oriented specimen do not possess such attributes. Special boundaries have been shown to be typically of low energy [13]. However, the criteria for establishing whether or not a particular boundary is of a sufficiently low energy configuration are by no means clear. Some authors specify that CSL boundaries characterized by low Σ values should be considered special, but often no upper limit on Σ is given. Bouchet and Priester [7] are more specific in their studies, indicating that Σ3 (disorientation axes: 111, 211), Σ5 (210, 310), Σ9 (221), Σ11 (311), Σ19a (331) and Σ27a (511) boundaries all show good segregation properties. However, they also conclude that the segregation properties are more dependent on the interplanar spacings parallel to the grain boundary plane than the Σ value. Ball sintering experiments [14] have also indicated that low Σ CSLs are low energy boundaries, and that grains might rotate slightly to low energy configurations, provided sufficient energy is available to overcome the relevant energy barriers. However, the depths of the energy cusps observed are not simply related to the Σ value. Lim and Raj [5] showed that random high angle boundaries develop cavities before lower Σ value boundaries, and that coherent Σ3 twin boundaries possess the greatest resistance of all boundary types to cavity formation. The evidence from experiments by Watanabe *et al.* [15], in which the misorientation dependence of grain boundary sliding was studied in zinc bicrystals, suggests that LABs and Σ9 CSLs possess greater resistance to sliding than other CSL-types, such as Σ15, Σ17 and Σ23. More recently, Lin and Pope [16] showed that the only boundary types which are strongly resistant to micro-crack nucleation in Ni_3Al are LABs and Σ3s. It is clear from this discussion that there is no definitive rationale by which grain boundaries may be labelled as special or otherwise. It should also be understood that in addition to the misorientation across a boundary (i.e. the Σ value), the orientation of the grain boundary plane also affects the degree of specialness.

As stated previously, the CSL model can be used to label boundaries according to grain misorientation, and that the energy of a particular boundary can be related, even if only qualitatively, to the Σ value adopted. Although it is possible to assign a Σ value to the boundary between any two adjacent grains, provided no upper limit is placed on Σ, this is not a physically realistic approach. A closer correlation can be made between the energy of a boundary and its Σ value if inexact CSL relationships are permitted. The deviation of a boundary from an exact CSL misorientation can be expressed as a parameter (v/v_m), where v is the angular rotation required to bring the boundary to the exact CSL misorientation, and v_m is the maximum permitted deviation, defined by the Brandon criterion [17]:

$$v_m = 15^\circ \Sigma^{-1/2} \quad (1)$$

An exact CSL misorientation possesses a characteristically lower energy than one for which a significant deviation value exists. A lower deviation parameter is therefore associated with a lower energy grain boundary configuration. The results obtained will be interpreted in terms of this deviation parameter, v/v_m.

The observations of changes in grain boundary geometries discussed above are a result of the system constantly endeavouring to minimize the boundary energy. At a temperature of 750 °C, insufficient thermal energy is imparted to the system to allow the activation energy for grain growth to be overcome. Therefore, energy minimization cannot be achieved, to any great degree, via the reduction of grain boundary area. All the energy imparted to the system during compressive strain is therefore available to provide the driving force for a recovery mechanism to produce more energetically favourable structures. The observed

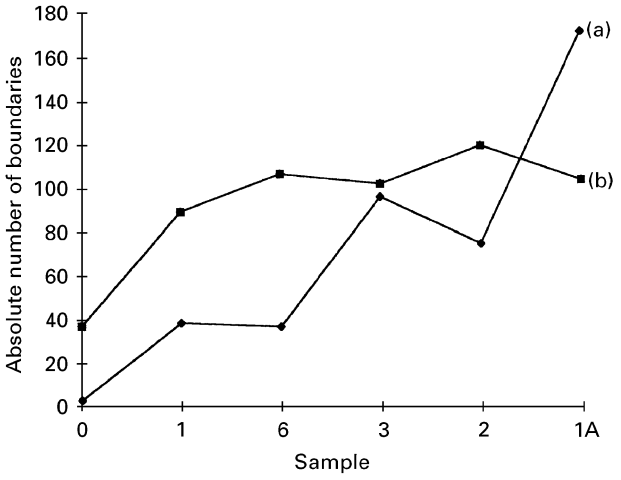

Figure 3 A comparison of the numbers of (a) coherent and (b) non-coherent Σ3 CSLs for each sample.

reduction in hardness with increased thermal treatment is evidence that the stored energy is being progressively expended. It is known that LABs and twin boundaries (Σ3) are more likely to have lower energy configurations than other CSL-types. Therefore, more attention will be paid to the study of LABs and Σ3s, because if sufficiently high levels of these boundaries can be introduced, the question as to whether various CSL-types are of sufficiently low energy to be considered special will not come into consideration.

There are two categories of Σ3 boundary. Coherent twins are known to lie on {111} planes, and are typically characterized in a 2-dimensional grain boundary network by a straight edged boundary between adjacent grains. They are often introduced during annealing [18]. Non-coherent Σ3 boundaries, in contrast, are often more curved in appearance. This is only a rule-of-thumb, and exceptions do occur. To be absolutely certain of the coherent nature of a particular boundary, a study must be made of the grain boundary plane (for example, see reference [19]).

In terms of the deviation parameter, an arbitrary threshold of $v/v_m = 0.2$ was chosen, such that a value below 0.2 inferred an annealing twin, and one above 0.2 identified a non-coherent Σ3. The selection of this threshold was checked by comparing the Σ3 population in sample 6 with the prediction of straight-edged Σ3 boundaries being coherent twins, and curved ones being non-coherent Σ3s. An 86% correlation was found, suggesting that the selection of this threshold is prudent.

Fig. 3 shows how the numbers of "coherent" and "non-coherent" Σ3s vary through the sample series. This indicates that while there are more non-coherent Σ3 boundaries than annealing twins in all but sample 1A, the increase in overall Σ3 numbers is almost entirely as a consequence of the increase in annealing twin numbers. After the reference sample (0), for which the number of grains studied is considerably less than that for the other specimens, the amount of non-coherent Σ3 grain boundaries increases only very slightly with increased thermal treatment. Conversely, the number of coherent twins can clearly be seen to increase with increased treatment.

A study was made to ascertain how the deviations from exact misorientation of various CSL-types vary with increased thermal treatment. Obviously, as the number densities of coherent Σ3 boundaries increase (with increased treatment), the overall deviation of the Σ3 CSL-types will decrease. However, the only other CSL-type for which any significant variation with treatment could be identified was the twin-related Σ9 boundary. The changes in the deviation parameter can be closely correlated with the number densities of annealing twins, and Σ9 boundaries themselves. There is no clear change in deviation parameter for sample 0, 1 and 6 (up to 12 h at 750 °C), but a significant drop occurs for sample 3 (24 h at 750 °C). This particular sample has been shown to possess a higher proportion of coherent twins, as well as having a greater number of Σ9s than all but sample 1A. The low deviation parameter threshold which, by the earlier definition ($v/v_m < 0.2$), contributes to the identification of an annealing twin, can therefore be seen to also correlate to twin related boundaries. A higher proportion of coherent twins will consequently result in a greater number of twin-related boundaries.

The number of annealing twins is considerably greater for sample 1A than for any other sample. The most obvious difference in the experimental matrix for this sample is the use of an air ambient during the entire treatment. The method of grain rotation discussed by Randle and Brown [12] involved energy minimization via the absorption of extrinsic grain boundary dislocations (EGBD), and is considered the most likely mechanism when grain boundary migration is not a possible method by which the boundary energy can be reduced. This is the case at a temperature of 750 °C. Thermal treatment in the presence of an air atmosphere will cause a diffusion of oxygen through the grain boundary network. If the concentration levels are sufficiently high the oxygen may become supersaturated, and on cooling precipitate in conjunction with low-level impurities present in Ni200, at defects such as the grain boundaries. The climb and glide actions by which the EGBDs are absorbed at the boundaries are thus disturbed, and hence the minimization of boundary energy by grain rotation is no longer the dominant mechanism. A more favourable process involves the formation of annealing twins in the manner described by Fullman and Fisher [18], which involves a decrease in the interfacial free energy as a result of the twinning operation. This is made more feasible because of the low stacking fault energy of nickel.

Although it is of great interest to discover the number of special boundaries in a material, and to ascertain methods for increasing their density, perhaps more importance should be attached to their connectivity in the grain boundary population. For example, intergranular fracture has been shown to occur preferentially at random boundaries rather than CSL-type boundaries [3], and so a triple junction devoid of random boundaries will act to check such a fracture. For a triple junction to be considered secure against,

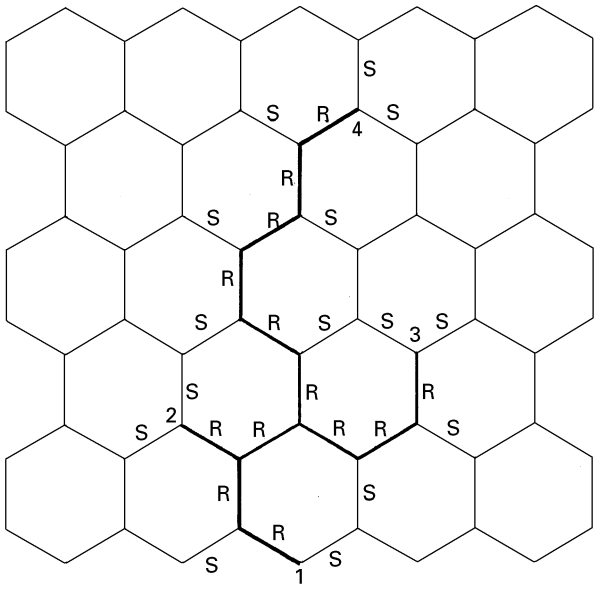

Figure 4 A schematic figure showing intergranular propagation of a crack through a grain boundary network of special (S) and random (R) boundaries. The crack is shown to propagate from triple junction 1, and is only arrested when a secure triple junction (labelled 2,3 and 4) is encountered.

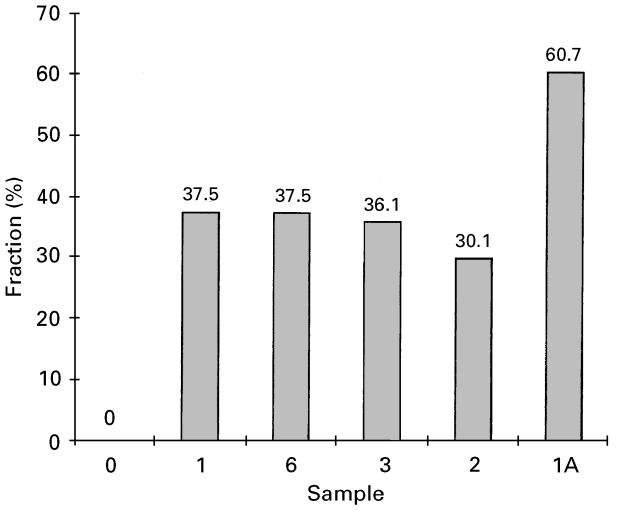

Figure 5 The fraction of triple junctions consisting of a coherent Σ3 boundary, and for which at least one other LAB, Σ3 or Σ9 boundary is present.

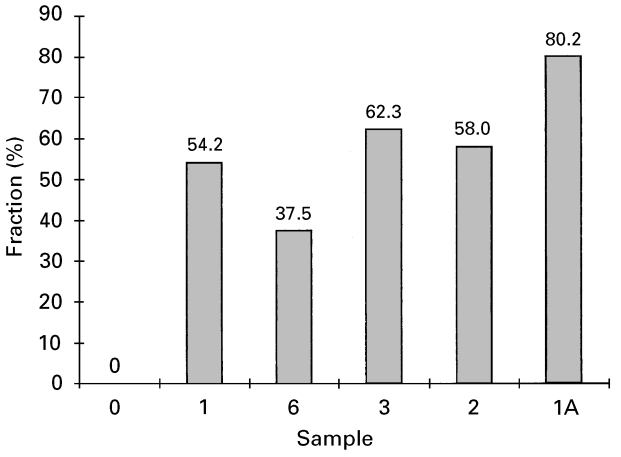

Figure 6 The fraction of triple junctions containing a coherent Σ3, for which the combination with a second Σ3 produces either a LAB or a Σ9, or for which combination with a Σ9 produces a Σ27.

for example, further propagation of a crack, only two of the three connected boundaries need to be of a low energy configuration. Although the third boundary, if random in nature, can provide a route by which the crack can reach the junction, further progress is arrested by the remaining two special boundaries. Fig. 4 shows schematically how the intergranular progress of a crack is made through a network of random and special grain boundaries. The crack propagates, travelling only along randomly oriented boundaries, until it reaches a "secure" triple junction. At such a junction its progress is terminated. Having eliminated the option of intergranular progress, the only mode of propagation available to the crack is transgranular. As this involves disturbing the single crystal nature of one of the adjoined grains, a high activation energy exists. Chiba *et al.* [1] have observed a change in the fracture mode in Ni_3Al from intergranular to transgranular, in the presence of high LAB and Σ3 densities, but this is not frequently observed. It is more common for a crack to cease propagating altogether if its intergranular path is blocked. Of course, further heat treatment at sufficiently high temperature can evoke the transgranular mode, rendering the crack active again.

As the density of coherent annealing twins is directly influenced by thermal treatment, and the presence of other related configurations is indirectly affected, there is a strong possibility that the connectivity of such low energy boundaries can be improved by such processing. Fig. 5 shows how many triple junctions, which are adjoined by at least one coherent twin, incorporate an additional low energy boundary, and can therefore be considered secure. It is clear from this work that no amount of treatment at 750 °C, after 6–7% compressive strain, can increase the number of secure triple junctions above approximately one third of those containing a coherent twin. However, the results for sample 1A show that over 60% of triple junctions, for which a coherent twin is incorporated, can be considered secure. Further to this observation, Fig. 2 shows that approximately 40% of all grain boundaries studied for sample 1A are characterized as Σ3s, and Fig. 3 reveals that over 60% of these are considered to be coherent in nature. Further to this study, triple junctions for which no coherent twins are incorporated, but that do consist of a non-coherent Σ3 plus another low energy boundary, were added to the statistics. The results were favourable, revealing that approximately 60% of triple junctions for which a Σ3 (coherent *or* non-coherent) is present can be considered secure. Therefore, whilst the number of coherent twins are more sensitive to thermal treatment, the presence of non-coherent Σ3s is also desirable.

To connectivity of Σ3 and Σ3-related boundaries seems to confirm the prediction of Ranganathan [8] that the product or quotient of the Σ values of two of the boundaries adjoining a triple junction will produce the Σ value of the third. Fig. 6 shows the

correlation with this relationship for the coherent Σ3 boundaries in the present series of samples. There are no relevant data for sample 0 (no coherent twins), but samples 1, 3 and 2 show between a 54–63% correlation. Sample 6 (12 h at 750 °C) only produces a 37.5% agreement, but the statistics for this sample are poor as there are only 24 data points. Sample 1A shows a correlation in excess of 80%, and good statistics exist because there are over 126 data points for this sample. Therefore, in addition to the numbers of secure triple junctions being controlled via strain annealing, their connectivity can also be strongly influenced.

5. Conclusions

Strain annealing can be seen to improve the proportions of special boundaries in Ni200 specimens. The increase in the coherent annealing twin population is by far the major influence on this effect. Annealing times of up to 24 h at 750 °C, after 6–7% compressive strain, improve the Σ3 densities. Further treatment at this temperature has no effect because the driving force provided to the system during the compressive strain stage has been expended. A preliminary surface oxidation treatment for 9 h at 500 °C has an even more dramatic effect on the coherent twin numbers, increasing them significantly. This is most likely due to oxygen diffusion and precipitation in the grain boundary network, hampering the grain rotation mechanisms by which boundary energy minimization is usually achieved at such temperatures, and rendering the twinning mechanism more favourable.

There does not seem to be a close, or obvious, correlation between the orientation texture of the grains and the misorientation texture of the grain boundaries. An oxidation pre-treatment does produce a characteristic texture, but one from which a prediction of the high Σ3 densities observed is not straightforward. It is also of great interest to note that this treatment results in a very high proportion of secure triple junctions, where a secure triple junction is one for which at least two of the adjoining interfaces are of the low energy type, that is, can be considered to possess special properties. The observed connectivity of such secure junctions will provide invaluable protection against many detrimental effects, for example, intergranular crack propagation.

It is clear that further work is necessary, not only to optimize the effects of thermomechanical treatment on the distribution of grain boundaries, but also to clarify the characteristics of a particular boundary which determine whether or not it can be classed as special.

Acknowledgements

The authors are grateful to Inco Alloys for providing the specimens, and acknowledge the financial assistance from the EPSRC (CT) and the Royal Society (VR).

References

1. A. CHIBA, S. HANADA, S. WATANABE, T. ABE and T. OBANA, *Acta Metall. Mater.* **42** (1994) 1733.
2. D. C. CRAWFORD and G. S. WAS, *J. Elect. Mic. Tech.* **19** (1991) 345.
3. T. WATANABE, *Metall. Trans.* **14A** (1983) 531.
4. G. PALUMBO and K. T. AUST, *Mater. Sci. Engng.* **A113** (1989) 139.
5. L. C. LIM and R. RAJ, *Acta Metall.* **34** (1986) 1183.
6. H. GRIMMER, W. BOLLMANN and D. H. WARRINGTON, *Acta Cryst.* **A30** (1974) 197.
7. D. BOUCHET and L. PRIESTER, *Scripta Metall.* **21** (1987) 475.
8. S. RANGANATHAN, *Acta Cryst.* **21** (1966) 197.
9. N-H. SCHMIDT, Commercially available software.
10. V. RANDLE, "Grain Boundary Geometry in Polycrystals," (Institute of Physics Publishing, Bristol, 1993).
11. L. ZUO and C. ESLING, *Scripta Metall. Mater.* **32** (1995) 937.
12. V. RANDLE and A. BROWN, *Phil. Mag. A* **59** (1989) 1075.
13. P. H. PUMPHREY, in "Grain Boundary Structure and Properties," edited by G. A. Chadwick and D. A. Smith (Academic Press, London, 1976).
14. G. HERRMANN, H. GLEITER and G. BARO, *Acta Metal.* **24** (1976) 353.
15. T. WATANABE, M. YAMADA, S. SHIMA and S. KARASHIMA, *Phil. Mag. A* **40** (1979) 667.
16. H. LIN and D. P. POPE, *Mater. Sci. Engng.* **A192**/**193** (1995) 394.
17. D. G. BRANDON, *Acta Metall.* **14** (1966) 1479.
18. R. L. FULLMAN and J. C. FISHER, *J. Appl. Phys.* **22** (1951) 1350.
19. V. RANDLE and D. DINGLEY, *Scripta Metall.* **23** (1989) 1565.

Received 7 June 1995
and accepted 21 May 1996